

Multidimensional Coherent Spectroscopy of Molecular Polaritons: Langevin Approach

Zhedong Zhang,^{1,2,*} Xiaoyu Nie,³ Danyuan Lei,⁴ and Shaul Mukamel^{5,6,†}

¹Department of Physics, City University of Hong Kong, Kowloon, Hong Kong SAR

²City University of Hong Kong, Shenzhen Research Institute, Shenzhen 518057, Guangdong, China

³Centre for Quantum Technologies, National University of Singapore, Singapore 117543

⁴Department of Materials Science and Engineering, City University of Hong Kong, Kowloon, Hong Kong SAR

⁵Department of Chemistry, University of California Irvine, Irvine, California 92697, United States

⁶Department of Physics and Astronomy, University of California Irvine, Irvine, California 92697, United States
(Dated: October 25, 2022)

We present a microscopic theory for nonlinear optical spectroscopy of N molecules in an optical cavity. A quantum Langevin analytical expression is derived for the time- and frequency-resolved signals accounting for arbitrary numbers of vibrational excitations. We identify clear signatures of the polariton-polaron interaction from multidimensional projections of the signal, e.g., pathways and timescales. Cooperative dynamics of cavity polaritons against intramolecular vibrations is revealed, along with a cross talk between long-range coherence and vibronic coupling that may lead to localization effects. Our results further characterize the polaritonic coherence and the population transfer that is slower.

Introduction.—Strong molecule-photon interaction has drawn considerable attention in recent study of molecular spectroscopy. New relaxation channels have been demonstrated to control fast electron dynamics and reaction activity [1–9]. Optical cavities create hybrid states between molecules and confined photons, known as polaritons [10–14]. Theoretically, this requires a substantial generalization of quantum electrodynamics (QED) into molecules containing many more degrees of freedom than atoms and qubits.

It has been demonstrated that light in a confined geometry can significantly alter the molecular absorption and emission signals [15–17]. The collective interaction between excitations of many molecules and photons is of fundamental importance, leading to interesting phenomena, e.g., superradiance and cooperative dynamics of polaritons [18–23]. In contrast to atoms whereby superradiance and cavity polaritons are well understood, molecular polaritons are more complex in theory and experiments. This arises from the complicated couplings between electronic and nuclear degrees of freedom, which possess new challenges for optical spectroscopy. Recently the absorption and fluorescence spectra are described by Holstein-Tavis-Cummings model [24, 25]. Exact diagonalization of the full Hamiltonian was used to calculate the optical responses, by only taking a few vibrational excitations into account [11, 26]. Here we focus on the polaritonic relaxation pathways involving the population and coherence dynamics, which are however open issues. Ultrafast spectroscopic technique has been used to monitor the dynamics of vibrational polaritons [22, 27, 28]. Time- and frequency-gated photon-coincidence counting was employed to monitor the many-body dynamics of cavity polaritons, making use of nonlinear interferometry [28, 29]. Polaritons reveal the effects of strongly modifying the energy harvesting and migration in chromophore aggregates, through novel control knobs not accessible by classical light [7, 13, 30–32]. Elaborate nonlinear optical measurements of molecular polaritons have demonstrated unusual correlation properties [33–35]. That calls for an extensive understanding of dark states with a high mode

density [36–42], nonlinearities and multiexciton correlations [43–47].

Previous spectroscopic studies of cavity polaritons were mostly based on wave function methods including nonadiabatic nuclear dynamics [48–50], Redfield theory and quantum chemistry simulations of low excitations [51–56]. Absorption and emission associated with multiple phonons and optically dark states depend on a strong polariton-polaron interaction, which raises a fundamental issue in cavity polaritons and however complicates the simulation of ultrafast spectroscopy.

In this Letter, we employ a quantum Langevin theory for time-frequency-resolved coherent spectroscopy of molecular polaritons. Analytical solution for multidimensional third-order spectroscopic signals is developed. The results reveal multiple channels and timescales of the cooperative relaxation of polaritons, and also the trade-off with dark states.

Langevin model for polaritons.—Given N identical molecules in an optical cavity, each has two energy surfaces corresponding to electronically ground and excited states, i.e., $|g_j\rangle$ and $|e_j\rangle$ ($j = 1, 2, \dots, N$), respectively. Electronic excitations forming excitons couple to intramolecular vibrations and to cavity photons, as depicted in Fig.1(b), and are described by the Holstein-Tavis-Cummings Hamiltonian

$$H = \sum_{n=1}^N \left[\Delta_n \sigma_n^+ \sigma_n^- + \omega_v b_n^\dagger b_n + g_n (\sigma_n^+ a + \sigma_n^- a^\dagger) + \delta_c a^\dagger a \right] \quad (1)$$

where $\Delta_n = \delta - \lambda \omega_v (b_n + b_n^\dagger)$ and δ denotes the detuning between excitons and external pulse field. $[\sigma_n^-, \sigma_m^+] = \sigma_n^- \delta_{nm}$. $\sigma_n^+ = |e_n\rangle \langle g_n|$ and $\sigma_n^- = |g_n\rangle \langle e_n|$ are the respective raising and lowering operators for the excitons in the n th molecule. b_n denotes the bosonic annihilation operator of the vibrational mode with a high frequency ω_v , in the n th molecule. a annihilates cavity photons. Each molecule has one high-frequency vibrational mode. In addition to the strong coupling to the single-longitudinal cavity mode, the molecules are subject to three temporally separated laser pulses whose electric fields $E_j(t - T_j)e^{-iv_j(t-T_j)}$; $j = 1, 2, 3$ described by

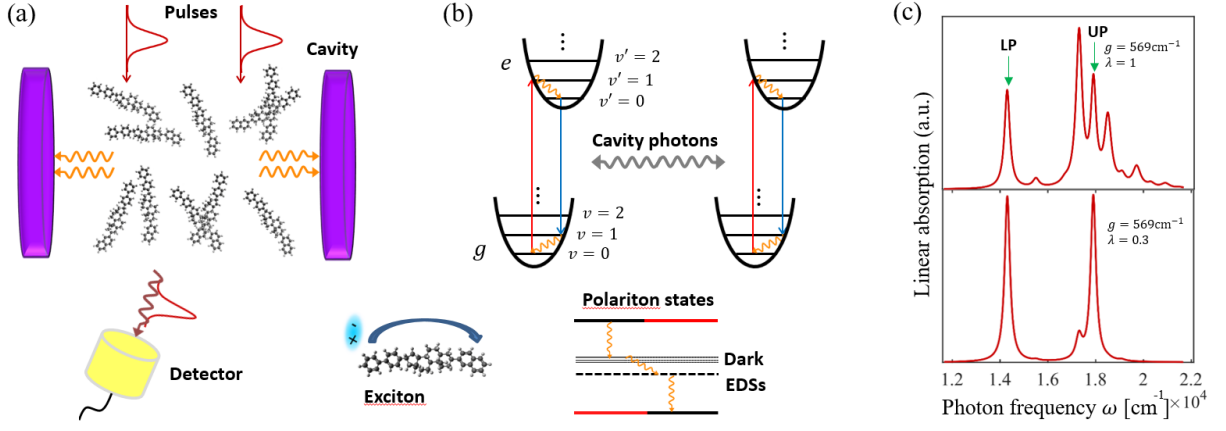


FIG. 1: Schematic of time-resolved spectroscopy for molecular polaritons. (a) Emission signal is collected along a certain direction, once the molecules are excited by laser pulses. (b) Exciton-photon interaction in molecules in the presence of vibronic coupling attached to individual molecule. This results in the dark states and emitter dark states (EDSs) weakly interacting with cavity, apart from the upper and lower polariton modes; Rich timescales and channels of excited-state relaxation are thus expected. (c) Linear absorption of molecular polaritons with 10 organic molecules in an optical cavity. The parameters are taken to be $\omega_D = 16113\text{cm}^{-1}$, $\tilde{\delta} = \delta_c = 0$, $\Gamma = 20\text{cm}^{-1}$, $\gamma = 1\text{cm}^{-1}$, $\gamma_c = 0.9\text{cm}^{-1}$, $\omega_v = 1200\text{cm}^{-1}$, typically from cyanine dyes [60].

$V(t) = \sum_{j=1}^3 \sum_{n=1}^N V_{j,n}(t) + \text{h.c.}$ with $V_{j,n}(t) = -\sigma_n^+ \Omega_j(t - T_j) e^{-i(v_j - v_3)t} e^{iv_j T_j}$ where $\Omega_j(t - T_j) = \mu_{eg} E_j(t - T_j)$ is the Rabi frequency with the j th pulse field and μ_{eg} is molecular dipole moment [57]. The full Hamiltonian is $H(t) = H + V(t)$, which yields the quantum Langevin equations (QLEs) for σ_n^- , a , b_n .

We incorporate the polaron transform via the displacement operator $D_n = e^{\lambda(b_n - b_n^\dagger)}$ into the QLE for the dressed operator $\tilde{\sigma}_n^- = \sigma_n^- D_n^\dagger$. This is to involve the exciton-vibration coupling to all orders, as it is normally moderate or strong. The QLEs for operators read a matrix form

$$\dot{\mathbf{V}} = -\hat{\mathbf{M}}\mathbf{V} + \mathbf{V}^{\text{in}}(t) + i \sum_{j=1}^3 \Omega_j(t - T_j) e^{iv_j T_j} e^{-i(v_j - v_3)t} \mathbf{W}_x \quad (2)$$

after a lengthy algebra, where the term $\propto (b_n - b_n^\dagger) = i\sqrt{2}p_n$ (p_n is the dimensionless momentum of nuclear) has been dropped due to the nuclear velocity much lower than electrons [59]. The vector $\mathbf{V} = [\tilde{\sigma}_1^-, \tilde{\sigma}_2^-, \dots, \tilde{\sigma}_N^-, a]^T$ involves $N + 1$ components, and $\mathbf{W}_x = [(2n_1 - 1)D_1^\dagger, \dots, (2n_N - 1)D_N^\dagger, 0]^T$, $n_l = \tilde{\sigma}_l^+ \tilde{\sigma}_l^-$. $\mathbf{V}^{\text{in}}(t) = [\sqrt{2}\gamma\tilde{\sigma}_1^{\text{in}}(t), \dots, \sqrt{2}\gamma\tilde{\sigma}_N^{\text{in}}(t), \sqrt{2}\gamma_c a^{\text{in}}(t)]^T$ groups the noise operators originated from exciton decay and cavity leakage. The matrix $\hat{\mathbf{M}}$ in Eq.(2) reads

$$\hat{\mathbf{M}} = \begin{pmatrix} i\tilde{\delta} + \gamma & 0 & \cdots & 0 & ig\sigma_1^z D_1^\dagger \\ 0 & i\tilde{\delta} + \gamma & \cdots & 0 & ig\sigma_2^z D_2^\dagger \\ \vdots & \vdots & \ddots & \vdots & \vdots \\ 0 & 0 & \cdots & i\tilde{\delta} + \gamma & ig\sigma_N^z D_N^\dagger \\ igD_1 & igD_2 & \cdots & igD_N & i\delta_c + \gamma_c \end{pmatrix}. \quad (3)$$

We solve for the vibration dynamics: $b_n(t) \approx e^{-(i\omega_n + \Gamma)t} b_n(0) + \sqrt{2}\Gamma \int_0^t e^{-(i\omega_n + \Gamma)(t-t')} b_n^{\text{in}}(t') dt'$, neglecting back influence from excitons, along the line of the stochastic Liouville equation

[22, 55]. Eq.(2) represents the dynamics of molecular polaritons. Perturbation theory of the molecule-field interaction $V(t)$ will be used and we will calculate two-dimensional photon emission signals by placing the detectors off the cavity axis, shown in Fig.1(a). These signals are governed by multipoint correlation functions of the dipole operators and the corresponding Green's functions, which are determined by the exact solution to the QLEs in Eq.(2).

The polariton emission.—We first present a general result for the emission spectrum of cavity polaritons. Subject to a probe pulse, Eq.(2) solves for the far-field dipolar radiation from molecules governed by the macroscopic polarization $P(t) = \mu_{eg}^* \sum_{i=1}^N \langle \sigma_{i,1}^-(t) \rangle$. We find the emission signal

$$P_E(\omega, T) = 2i|\mu_{eg}|^2 \sum_{i=1}^N \sum_{l=1}^N \int_{-\infty}^{\infty} dt \int_0^t d\tau e^{i\omega t} E(\tau - T) \times e^{-iv(\tau-T)} \langle G_{il}(t - \tau) n_l(\tau) D_l^\dagger(\tau) D_i(t) \rangle \quad (4)$$

where $G(t) = \mathcal{T} e^{-\int_0^t \hat{\mathbf{M}} dt'}$ is the free propagator without pulse actions. We note that, from the dressed excited-state populations $n_l(\tau) D_l^\dagger(\tau)$, the cavity polaritons of molecules undergo a dynamics against the local fluctuations from polaron effect. The polaron-induced localization as a result of dark states will compete with the cooperative dynamics of polaritons. These can be visualized from the emission signal, which will thus be a real-time monitoring of polariton dynamics through pulse shaping and grating. More advanced information will be elaborated by the multidimensional projections of the signals.

Linear absorption.—Assuming $\omega_v/T_b \gg 1$ that applies for organic molecules at room temperature, the vibrational correlation functions can be evaluated within vacuum state. Using Eq.(2), the absorption spectra reads $S_A(\omega) = \sum_{i,l=1}^N \sum_{m=0}^{\infty} S_m^A \delta_{il}^m \text{Re}[\mathcal{G}_{il}(\omega - \xi_m^*)]$ and $S_m^A = e^{-\lambda^2} \lambda^{2m}/m!$

is the Franck-Condon factor. $\xi_m = m(\omega_v + i\Gamma)$ and $\mathcal{G}_{mm}(\Omega) = \int_0^\infty G_{mm}(t)e^{i\Omega t}dt$ is the Fourier component of the propagator $G(t)$. $S_A(\omega)$ resolves the lower polariton (LP) and upper polariton (UP) $\omega_{\text{LP/UP}}$, EDSs $\omega_D + m\omega_v$ decoupled from cavity photons while the dark states ω_D are not visible. To see these closely, we assume $\gamma = \gamma_c$, $\tilde{\delta} = \delta_c = 0$. The peak intensities can be thus found $S_A(\omega_D + m\omega_v)/S_A(\omega_{\text{LP/UP}}) \approx 2(\lambda^{2m}/m!)(\gamma_{\text{LP/UP}}/m\Gamma)$ and $S_A(\omega_{\text{LP/UP}} + m\omega_v)/S_A(\omega_{\text{LP/UP}}) \approx 0$ when $N \gg 1$. The modes at $\omega_{\text{LP/UP}} + m\omega_v$ are hard to observe. Yet the EDSs at $\omega_D + m\omega_v$ may be of comparable intensities with polariton modes. Such spectral-line properties will be shown to be generally true in the time-resolved spectroscopic signals.

Fig.1(c,up) illustrates the absorption spectra where the LP and UP are prominent from the peaks at 14300cm^{-1} and 17900cm^{-1} separated by $2g\sqrt{N}$. In between, we can observe an extra peak at $\omega_D + \omega_v$ supporting an EDS decoupled from cavity photons and the large oscillator strength owing to the density of states $\sim N$. Fig.1(c,down) shows that the EDSs are masked by the Rabi splitting for weaker vibronic coupling. This, as a benchmark to the strong-coupling case, elaborate the effect of vibronic coupling against the collective coupling to cavity photons. The localization nature of the EDSs is thus indicated from eroding the cooperativity between molecules, which will be elaborated in time-resolved spectroscopy.

2D polariton spectroscopy.—To have multidimensional projections of the emission signal, a sequential laser pulses have to interact with the molecular polaritons. As the first two pulses create excited-state populations and coherences $n_{i,2}(t) = \sigma_{i,1}^+(t)\sigma_{i,1}^-(t)$ where the 1st-order correction $\sigma_{i,1}^\pm$ is calculated from Eq.(2), we find

$$n_{i,2}(t)D_i^\dagger(t) = \sum_{j=1}^N \sum_{j'=1}^N \iint_0^t dt'' dt' \mathcal{E}_1^*(t' - T_1) \mathcal{E}_2(t'' - T_2) \times G_{ij'}^*(t - t') G_{ij}(t - t'') D_j(t') D_j^\dagger(t'') D_i^\dagger(t). \quad (5)$$

The 3rd-order correction to the polarization follows Eq.(4) when the third pulse serves as probe. Given the time-ordered pulses, the transition pathways are selective resulting from the term cancellation. Inserting Eq.(5) into Eq.(4), we therefore proceed to the far-field polarization for the emission along the direction $\mathbf{k}_1 = -\mathbf{k}_1 + \mathbf{k}_2 + \mathbf{k}_3$, i.e., $P(t) = \mu_{eg}^* \sum_{i=1}^N \langle \sigma_{i,3}^-(t) \rangle$ which yields

$$P(\omega) = 2i \sum_{i,l=1}^N \sum_{j,j'=1}^N \iiint_0^\infty dt dt' dt'' dt' e^{i\omega t} \mathcal{E}_3(\tau - T_3) \times \mathcal{E}_2(t'' - T_2) \mathcal{E}_1^*(t' - T_1) \langle 0 | G_{il}(t - \tau) G_{ij'}^*(\tau - t') \times G_{ij}(\tau - t'') D_j(t') D_j^\dagger(t'') D_l^\dagger(\tau) D_l(t) | 0 \rangle \quad (6)$$

where the four-point correlation function of vibrations $\langle 0 | D_j(t') D_j^\dagger(t'') D_l^\dagger(\tau) D_l(t) | 0 \rangle$ has to be evaluated explicitly. The 2D signal is usually detected via a reference beam as a local oscillator interfering with the emission. This

leads to the heterodyne-detected signal $S_{2\text{D}}(\Omega_3, T, \Omega_1) = \text{Im} \int_0^\infty E_{\text{LO}}^*(\Omega_3) P(\Omega_3) e^{i\Omega_1 \tau} d\tau$ with the Fourier transform against the 1st delay $\tau = T_2 - T_1$, where $E_{\text{LO}}(\Omega_3)$ is the Fourier component of the local oscillator field. In general, calculating the signal with Eq.(6) is hard due to the integrals over pulse shapes. The procedures can be simplified by invoking the *impulsive approximation* such that the pulse is shorter than the dephasing and solvent time scales. We further consider the few-photon cavity that draws much attention in recent experiments, and notice the vibronic coupling predominately accounted by the polarons. The most significant terms may be remained, allowing the approximation $g\sigma_l^\pm D_l^\dagger \approx gD_l^\dagger \approx g$ in Eq.(3). The higher-order corrections will be presented elsewhere. We obtain an analytical solution to the 2D polariton signal (2DPS), up to a real constant

$$S(\Omega_3, T, \Omega_1) = ie^{i\phi} \sum_{i,l=1}^N \sum_{j,j'=1}^N \sum_{p=1}^{N+1} \sum_{\{m\}=0}^\infty S_{\{m\}}^\lambda \delta_{ij'}^{m_1} \delta_{il}^{m_2} \delta_{jl}^{m_3} \delta_{j'l}^{m_4} \times \delta_{ij}^{m_5} \delta_{ij'}^{m_6} (-1)^{m_3+m_6} \mathcal{G}_{il}(\Omega_3 + \xi_{m_2+m_5+m_6}) G_{lp}^*(T) G_{lj}(T) \times e^{i\xi_{m_3+m_4+m_5+m_6} T} \mathcal{G}_{pj'}^*(-\Omega_1 - \xi_{m_1+m_4+m_6}) \quad (7)$$

subsequently from Eq.(6), where $S_{\{m\}}^\lambda = \prod_{s=1}^6 S_{m_s}^\lambda$ and ϕ encodes the global phase from the four classical pulses. Details of the derivation of the signals via QLEs are given in Supplemental Material [59].

Simulations.—We have simulated the 2DPS to study polariton, exciton and polaron dynamics from the analytical solutions. We set $g\sqrt{N}/\omega_v = 1.5$ for strong coupling.

The lower and upper rows in Fig.2 illustrate the 2DPS respectively for $N = 1$ and 10 molecules with fixed Rabi frequency $2g\sqrt{N}$. For 10 molecules in cavity, the signal reveals the real-time population transfer and coherence dynamics between polaritons and EDSs. The EDSs, however, cannot be resolved when one molecule coupled to cavity only. This is evident by the absence of the peaks at $\Omega_{1,3} = \omega_D \pm n\omega_v$ ($n = 0, 1, 2, \dots$) in the lower row, compared with the upper row. The 2DPS for $N = 1$ can monitor the states at $\omega_{\text{UP}} - \text{integer} \times \omega_v$ and their population transfer as well as coherence with the polariton states, as seen from the variation of the cross peaks, for example, at $(\Omega_1 = \omega_{\text{UP}} - n\omega_v, \Omega_3 = \omega_{\text{UP}} - m\omega_v), m \neq n$ with the time delay T . We will present more details about the polariton dynamics against the EDSs next.

Fig.2(a) shows the 2D signal at $T = 0$, from which the LP and UP states can be observed, evident by the two diagonal peaks at $\omega \pm g\sqrt{N}$. The cross peaks may result from the coherence and the polariton-polaron coupling, since energy and dephasing are not allowed at $T = 0$. The former is due to the broadband nature of pump pulses while the latter is responsible for the change of phonon numbers associated with optical transitions. To have a closer look, we notice the states at $\Omega_1 = 14300, 17300$ and 17900cm^{-1} , after the absorbing energy from the pump pulse. These agree with the absorbance in Fig.1(c,up). The cross peaks imposing $\Omega_1 - \Omega_3 = \text{integer} \times \omega_v$ indicates the population of the EDSs which decouple from

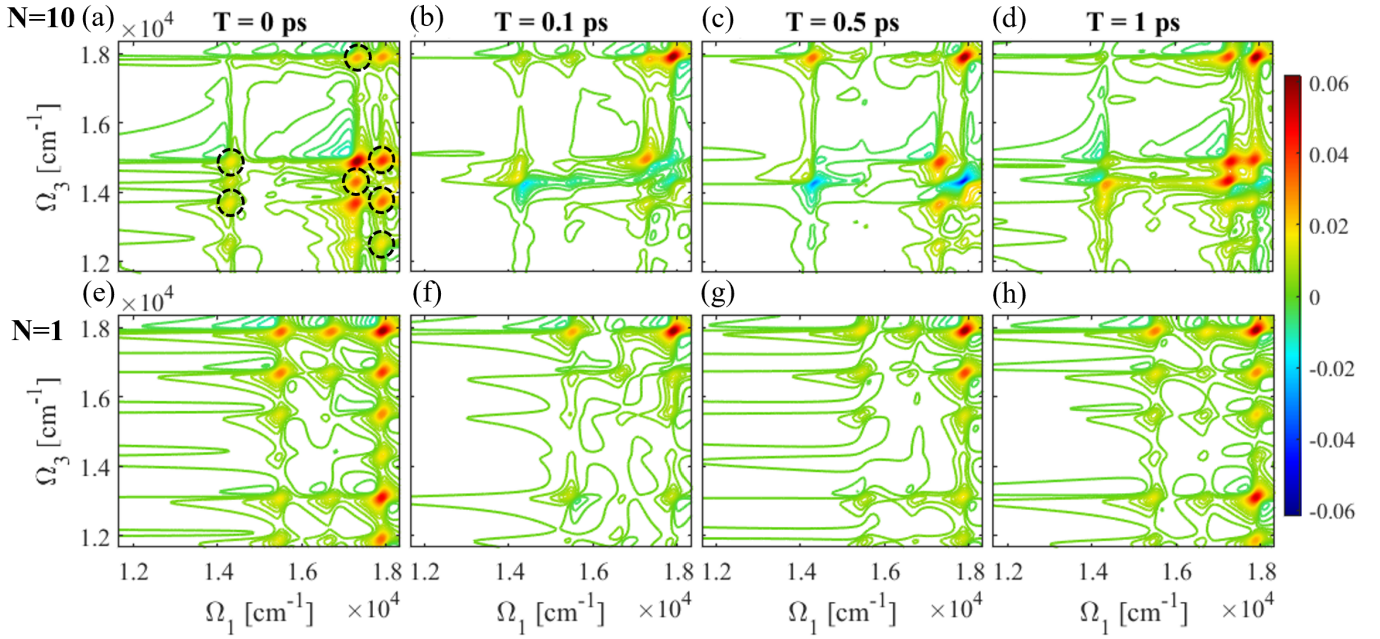


FIG. 2: 2D time- and frequency-resolved signal for molecular polaritons where (up) $N = 10$ organic molecules and (down) $N = 1$ organic molecule. T is varied, denoting the delay between the 2nd and the probe laser pulses. Horizontal and vertical axis are for absorption and emission frequencies, respectively. $\lambda = 1$ and $g\sqrt{N}/\omega_v = 1.5$. Other parameters are the same as Fig.1.

cavity photons and radiate phonons when emitting photons, evident by those at $(\Omega_1 = 17300\text{cm}^{-1}, \Omega_3 = 14900\text{cm}^{-1})$ and $(\Omega_1 = 17300\text{cm}^{-1}, \Omega_3 = 13700\text{cm}^{-1})$. The EDSs erode eroding molecular cooperativity and are highly degenerated, having the frequency $\omega_D \pm n\omega_v; n = 1, 2, \dots$. The cross peaks with $\Omega_1 - \Omega_3 \neq \text{integer} \times \omega_v$ as circled in Fig.2(a), come from the coherences quantified by the off-diagonal elements of the density matrix. For instance, the one at $(\Omega_1 = 17900\text{cm}^{-1}, \Omega_3 = 14900\text{cm}^{-1})$ resolves the coherence $\rho_{\omega_D - \omega_v, \omega_{\text{UP}}}(T)$. The peaks associated with EDSs in both absorption spectrum and the 2D signal $S_{2D}(\Omega_3, 0, \Omega_1)$ manifest in the steady state of molecular ensemble the role of local fluctuations that erodes the cooperative motion of exciton polaritons. This incredibly differs from previous studies showing the dynamical breakdown of the polariton-induced cooperativity of molecules by solvent motion which does not affect the polaritons significantly in the absorption spectrum, apart from the line broadening [22].

When the delay between the 2nd and probe pulses varies, Fig.2(b) show the fast decay of the coherence produced from the first two broadband pulses. This can be seen prominently from the decreasing intensities of the cross peaks with $\Omega_1 - \Omega_3 \neq \text{integer} \times \omega_v$, compared to Fig.2(a). From Fig.2(b), nevertheless, one can observe the cross peak at $(\Omega_1 = 17900\text{cm}^{-1}, \Omega_3 = 14900\text{cm}^{-1})$ whose intensity increases after a rapid decay with the delay T . This describes the down-hill energy transfer from UP to the EDS $\omega = \omega_D - \omega_v = 14900\text{cm}^{-1}$, following a fast dephasing. An energy transfer to LP is elucidated as well, from the growth of the cross peak at $(\Omega_1 = 17900\text{cm}^{-1}, \Omega_3 = 14300\text{cm}^{-1})$. Similarly, the energy transfer pathway from the EDS $\omega = \omega_D + \omega_v = 17300\text{cm}^{-1}$

to the LP can be observed within about 300fs. Observing the weak intensity along with a slow growth at the cross peaks $(\Omega_1 = 17900\text{cm}^{-1}, \Omega_3 = \omega_D - n\omega_v)$ in Fig.2(b,c), the molecular system is slightly localized from the UP state within $\sim 500\text{fs}$ because of the weak populations of EDSs. Within a longer timescale $T > 500\text{fs}$, Fig.2(c,d) evidence that the energy flowing from UP and the state $\omega = \omega_D + \omega_v = 17300\text{cm}^{-1}$ to the EDS $\omega = \omega_D - \omega_v = 14900\text{cm}^{-1}$ dominates, leading to strong localization of the UP state. This can be neatly understood from the Fermi-Golden rule $\Gamma_{i \rightarrow f} = 2\pi | \langle f | V | i \rangle |^2 N_i D_f$ by noting a larger number of EDSs than polaritons. From the slice $\Omega_1 = \omega_D + \omega_v = 17300\text{cm}^{-1}$ in which the system can be pumped to the state at $\omega_D + \omega_v$ by the first two pulses, the system tends to be alternatively delocalized within a longer timescale $T > 500\text{fs}$, seen from Fig.2(c,d) showing the strong peak intensity at LP state that indicates the population transferred considerably.

Moreover, one notes in Fig.2 that most of the cross peaks appear below the diagonal. This results from the low temperature assumed in our model, i.e., $\omega_v/T_b \gg 1$ so that the vibration modes are at vacuum initially before the pulse actions. During the first 250fs, the fast decay of the cross peak at $(\Omega_1 = 14300\text{cm}^{-1}, \Omega_3 = 14900\text{cm}^{-1})$ monitors the dephasing of the coherence $\rho_{\omega_D - \omega_v, \omega_{\text{LP}}}(T)$. The population transfer from the LP state to the EDS $\omega = \omega_D - \omega_v = 14900\text{cm}^{-1}$ follows when the delay T becomes longer, as indicated from the cross peak at $(\Omega_1 = 14300\text{cm}^{-1}, \Omega_3 = 14900\text{cm}^{-1})$ that increases within about 750fs. Besides, the cross peak at $(\Omega_1 = 14300\text{cm}^{-1}, \Omega_3 = 17900\text{cm}^{-1})$ shows up weakly within about 500fs, as depicted in Fig.2(c). A small portion of energy

transferred from the LP state to the UP state is thus indicated. This may be attributed to the rapid energy exchange between the polariton and vibration modes, yielding a cascading migration of populations between two polariton modes within a short timescale. In longer timescales, such behavior is expected to deplete.

Relation to the pump-probe signal.—The pump-probe signal can be readily obtained by letting $T_1 = T_2$ in Eq.(6) and accounting for the non-rephasing component. The signal reads $S_{pp}(\omega, T) = \text{Im}[E_3^*(\omega)P(\omega)]$ and some algebra gives

$$S_{pp}(\omega, T) = \sum_{i,l=1}^N \sum_{j,j'=1}^N \sum_{\{m\}=0}^{\infty} S_{\{m\}}^{\lambda} \delta_{il}^{m_1} (\delta_{j'l} - \delta_{jl})^{m_2} (\delta_{ij} - \delta_{ij'})^{m_3} \times \text{Re} \left[\mathcal{G}_{il}(\omega + \xi_{m_1+m_3}) G_{lj'}^*(T) G_{lj}(T) e^{i\xi_{m_2+m_3}T} \right] \quad (8)$$

under the *impulsive approximation*. The broadband nature of the ultrashort pulses smears out the mode selectivity in the absorption of molecular polaritons, whereas the time grating makes the emission spectrally resolved. Similar as the 2DPS, the LP and UP modes separated by $2g\sqrt{N}$ as well as the EDSs at $\omega = \omega_D - m\omega_v$ can be resolved in $S_{pp}(\omega, T)$. As varying the time delay, the spectral-line intensity $S_{pp}(\omega_{UP/LP}, T)$ shows a phase difference from the $S_{pp}(\omega_D - m\omega_v, T)$, associated with different damping rates that are responsible for the incoherent channels of relaxations. The low spectral resolution with the absorption process, however, makes the pump-probe signal not capable of unveiling advanced information about the polariton dynamics and dark states, e.g., relaxation pathways and timescales. More details are given in SM [59].

Summary and outlook.—The microscopic theory of multi-dimensional spectroscopy for the molecular polaritons was developed, using the quantum Langevin equation capable of polariton-polaron interactions with high excitation number. Rich information about the fast-evolving dynamics of polaritons and dark states and their couplings can be readily visualized in the 2DPS, i.e., pathways and timescales. Our work manifests the ultrafast polariton-polaron interaction in molecules, resolving the EDSs against the polariton dynamics. This falls into a different category from the cavity QED for atoms, in which no relaxation between superradiant and subradiant states could be observed [61–63]. Understanding the collective nature of molecular polaritons is significant for the community to gain more details about the diverse phenomena afforded by the polaritons in complex materials. This knowledge may help in the design of cavity-coupled heterostructures in visible regime and in polariton chemistry.

Z.D.Z. gratefully acknowledges the support of ARPC-CityU new research initiative/infrastructure support from central (No. 9610505), the Early Career Scheme from Hong Kong Research Grants Council (No. 21302721) and the National Science Foundation of China (No. 12104380). D.L. gratefully acknowledges the support of the National Science Foundation of China, the Excellent Young Scientist Fund (No. 62022001). S.M. thanks the support of the National Science

Foundation (No. CHE-1953045) and of the U.S. Department of Energy, Office of Science, Basic Energy Sciences, under Award No. DE-SC0022134.

* zzhan26@cityu.edu.hk

† smukamel@uci.edu

- [1] A. Thomas, J. George, A. Shalabney, M. Dryzhakov, S. J. Varma, *et al.*, *Angew. Chem. Int. Ed.* **55**, 11462-11466 (2016)
- [2] J. Hutchison, T. Schwartz, C. Genet, E. Devaux and T. W. Ebbesen, *Angew. Chem.* **124**, 1624-1628 (2012)
- [3] A. D. Dunkelberger, B. T. Spann, K. P. Fears, B. S. Simpkins and J. C. Owrutsky, *Nat. Commun.* **7**, 13504-13513 (2016)
- [4] X. Li, A. Mandal and P. Huo, *Nat. Commun.* **12**, 1315-1323 (2021)
- [5] F. Herrera and F. C. Spano, *Phys. Rev. Lett.* **116**, 238301-238305 (2016)
- [6] L. Martinez-Martinez, R. Ribeiro, J. Campos-Gonzalez-Angulo and J. Yuen-Zhou, *ACS Photonics* **5**, 167-176 (2018)
- [7] D. M. Coles, N. Somaschi, P. Michetti, C. Clark, P. G. Lagoudakis, P. G. Savvidis and D. G. Lidzey, *Nat. Mater.* **13**, 712-719 (2014)
- [8] M. Kowalewski, K. Bennett and S. Mukamel, *J. Phys. Chem. Lett.* **7**, 2050-2054 (2016)
- [9] J. Galego, F. J. Garcia-Vidal and J. Feist, *Nat. Commun.* **7**, 13841-13846 (2016)
- [10] S. Aberra Guebrou, C. Symonds, E. Homeyer, J. C. Plenet, Yu. N. Gartstein, V. M. Agranovich and J. Bellessa, *Phys. Rev. Lett.* **108**, 066401-066405 (2012)
- [11] F. C. Spano, *J. Chem. Phys.* **142**, 184707-184718 (2015)
- [12] A. Shalabney, J. George, J. Hutchison, G. Pupillo, C. Genet and T. W. Ebbesen, *Nat. Commun.* **6**, 5981-5986 (2015)
- [13] J. Flick, M. Ruggenthaler, H. Appel and A. Rubio, *Proc. Natl. Acad. Sci. U.S.A.* **114**, 3026-3034 (2017)
- [14] J. M. Raimond, M. Brune and S. Haroche, *Rev. Mod. Phys.* **73**, 565-582 (2001)
- [15] D. Wang, *et al.*, *Nat. Phys.* **15**, 483-489 (2019)
- [16] E. Hulkko1, S. Pikker, V. Tiainen, R. H. Tichauer, G. Groenhof and J. J. Toppari, *J. Chem. Phys.* **154**, 154303-154312 (2021)
- [17] K. Georgiou, R. Jayaprakash, A. Askitopoulos, D. M. Coles, P. G. Lagoudakis and D. G. Lidzey, *ACS Photonics* **5**, 4343-4351 (2018)
- [18] M. Tavis and F. W. Cummings, *Phys. Rev.* **170**, 379-384 (1968)
- [19] M. Gross and S. Haroche, *Phys. Rep.* **93**, 301-396 (1982)
- [20] M. O. Scully and A. A. Svidzinsky, *Science* **325**, 1510-1511 (2009)
- [21] F. C. Spano, J. R. Kuklinski and S. Mukamel, *Phys. Rev. Lett.* **65**, 211-214 (1990)
- [22] Z. D. Zhang, K. Wang, Z. Yi, M. S. Zubairy, M. O. Scully and S. Mukamel, *J. Phys. Chem. Lett.* **10**, 4448-4454 (2019)
- [23] F. J. Garcia-Vidal, J. Feist and J. del Pino, *New J. Phys.* **17**, 053040-053050 (2015)
- [24] F. Herrera and F. C. Spano, *Phys. Rev. Lett.* **118**, 223601-223606 (2017)
- [25] M. Reitz, C. Sommer and C. Genes, *Phys. Rev. Lett.* **122**, 203602-203607 (2019)
- [26] F. C. Spano and C. Silva, *Ann. Rev. Phys. Chem.* **65**, 477-500 (2014)
- [27] B. Xiang, *et al.*, *Proc. Natl. Acad. Sci. U.S.A.* **115**, 4845-4850 (2018)
- [28] K. E. Dorfman and S. Mukamel, *Proc. Natl. Acad. Sci. U.S.A.*

- 115**, 1451-1456 (2018)
- [29] Z. D. Zhang, P. Saurabh, K. E. Dorfman, A. Debnath and S. Mukamel, *J. Chem. Phys.* **148**, 074302-074314 (2018)
- [30] M. Kowalewski, K. Bennett and S. Mukamel, *J. Phys. Chem. Lett.* **7**, 2050-2054 (2016)
- [31] Z. D. Zhang, T. Peng, X. Y. Nie, G. S. Agarwal and M. O. Scully, arXiv:2106.10988v2 [quant-ph]
- [32] T. W. Ebbesen, *Acc. Chem. Res.* **49**, 2403-2412 (2016)
- [33] F. Herrera, B. Peropadre, L. A. Pachon, S. K. Saikin and A. Aspuru-Guzik, *J. Phys. Chem. Lett.* **5**, 3708-3715 (2014)
- [34] B. Xiang, R. F. Ribeiro, Y. Li, A. D. Dunkelberger, B. B. Simpkins, J. Yuen-Zhou and W. Xiong, *Sci. Adv.* **5**, eaax5196 (2019)
- [35] B. Xiang, J. Wang, Z. Yang and W. Xiong, *Sci. Adv.* **7**, eabf6397 (2021)
- [36] Z. D. Zhang and S. Mukamel, *Chem. Phys. Lett.* **683**, 653-657 (2017)
- [37] M. A. Zeb, P. G. Kirton and J. Keeling, *ACS Photonics* **5**, 249-257 (2018)
- [38] J. Galego, F. J. Garcia-Vidal and J. Feist, *Phys. Rev. X* **5**, 041022-041035 (2015)
- [39] J. Flick and P. Narang, *Phys. Rev. Lett.* **121**, 113002-113007 (2018)
- [40] L. Lacombe, N. M. Hoffmann and N. T. Maitra, *Phys. Rev. Lett.* **123**, 083201-083206 (2019)
- [41] A. Csehi, Á. Vibók, G. J. Halász and M. Kowalewski, *Phys. Rev. A* **100**, 053421-053429 (2019)
- [42] M. Du and J. Yuen-Zhou, *Phys. Rev. Lett.* **128**, 096001-096007 (2022)
- [43] P. Saurabh and S. Mukamel, *J. Chem. Phys.* **144**, 124115-124120 (2016)
- [44] J. Gu, *et al.*, *Nat. Commun.* **12**, 2269-2275 (2021)
- [45] S. Mukamel, *J. Chem. Phys.* **145**, 041102-041104 (2016)
- [46] J.-H. Zhong, *et al.*, *Nat. Commun.* **11**, 1464-1473 (2020)
- [47] V. M. Axt and S. Mukamel, *Rev. Mod. Phys.* **70**, 145-174 (1998)
- [48] M. Kowalewski, K. Bennett and S. Mukamel, *J. Chem. Phys.* **144**, 054309-054316 (2016)
- [49] J. Flick, H. Appel, M. Ruggenthaler and A. Rubio, *J. Chem. Theory Comput.* **13**, 1616-1625 (2017)
- [50] M. Gudem and M. Kowalewski, *J. Phys. Chem. A* **125**, 1142-1151 (2021)
- [51] H.-P. Breuer and F. Petruccione, *The Theory of Open Quantum Systems* (Oxford University Press, Oxford, 2002)
- [52] N. T. Phuc, *J. Chem. Phys.* **155**, 014308-014313 (2021)
- [53] F. Herrera and F. C. Spano, *Phys. Rev. A* **95**, 053867-053890 (2017)
- [54] R. Saez-Blazquez, J. Feist, E. Romero, A. I. Fernandez-Domínguez and F. J. García-Vidal, *J. Phys. Chem. Lett.* **10**, 4252-4258 (2019)
- [55] Y. Tanimura, *J. Phys. Soc. Jpn.* **75**, 082001-082039 (2006)
- [56] R. F. Ribeiro, *et al.*, *J. Phys. Chem. Lett.* **9**, 3766-3771 (2018)
- [57] We have adopted the Condon approximation that μ_{eg} is independent of the nuclear coordinates [58].
- [58] S. Mukamel, *Principles of Nonlinear Optical Spectroscopy* (Oxford University Press, Oxford, 1999)
- [59] See Supplemental Material for a detailed description of 2D coherent signal with quantum Langevin equation.
- [60] C. A. Guarín, J. P. Villabona-Monsalve, R. López-Arteaga and J. Peon, *J. Phys. Chem. B* **117**, 7352-7362 (2013)
- [61] D. Pavolini, A. Crubellier, P. Pillet, L. Cabaret and S. Liberman, *Phys. Rev. Lett.* **54**, 1917-1920 (1985)
- [62] W. Guerin, M. O. Araujo and R. Kaiser, *Phys. Rev. Lett.* **116**, 083601-083605 (2016)
- [63] R. E. Evans, *et al.*, *Science* **362**, 662-665 (2018)

Multidimensional Coherent Spectroscopy of Molecular Polaritons: Langevin Approach

Zhedong Zhang,^{1,2,*} Xiaoyu Nie,³ Danyuan Lei,⁴ and Shaul Mukamel^{5,6,†}

¹*Department of Physics, City University of Hong Kong, Kowloon, Hong Kong SAR*

²*City University of Hong Kong, Shenzhen Research Institute, Shenzhen 518057, Guangdong, China*

³*Centre for Quantum Technologies, National University of Singapore, Singapore 117543*

⁴*Department of Materials Science and Engineering,*

City University of Hong Kong, Kowloon, Hong Kong SAR

⁵*Department of Chemistry, University of California Irvine, Irvine, California 92697, United States*

⁶*Department of Physics and Astronomy, University of California Irvine, Irvine, California 92697, United States*

(Dated: October 25, 2022)

The math details in addition to the conclusions delivered in main text are provided. Meanwhile, some supplemental results on multidimensional spectroscopy of cavity polaritons are shown, in support of the main text.

LANGEVIN MODEL FOR POLARON POLARITONS

Given N identical molecules in an optical cavity, the Holstein-Tavis-Cummings Hamiltonian reads

$$H_0 = \sum_{n=1}^N [\delta_n \sigma_n^+ \sigma_n^- + \omega_{\text{vib}} b_n^\dagger b_n - \lambda_n \omega_{\text{vib}} \sigma_n^+ \sigma_n^- (b_n + b_n^\dagger) + g_n (\sigma_n^+ a + \sigma_n^- a^\dagger)] + \delta_c a^\dagger a \quad (1)$$

in the rotating frame of photons, where σ_n^+ is the raising operator leading to electronic excitation of the n th molecule. b_n denotes the annihilation operator of the vibrational mode having the frequency ω_{vib} . a annihilates a photon in cavity and $\delta_n = \omega_n - v$ denotes the detuning between excitons and external classical field. In the presence of the classical laser pulses, the full Hamiltonian is $H = H_0 + V(t)$ and

$$V(t) = - \sum_{n=1}^N \sum_{j=1}^3 [\sigma_n^+ \Omega_j(t - T_j) e^{-i(v_j - v_3)t} e^{iv_j T_j} + \sigma_n^- \Omega_j^*(t - T_j) e^{i(v_j - v_3)t} e^{-iv_j T_j}] \quad (2)$$

with the Rabi frequency $\Omega_j(t - T_j) = \mu_{eg} E_j(t - T_j)$. The quantum Langevin equations (QLEs) for operators are of the form

$$\dot{\sigma}_n^- = -(i\delta + \gamma) \sigma_n^- + i\lambda \omega_{\text{vib}} \sigma_n^- (b_n + b_n^\dagger) - ig \sigma_n^z a - i \sum_{j=1}^3 \sigma_n^z \Omega_j(t - T_j) e^{-i(v_j - v_3)t} e^{iv_j T_j} + \sqrt{2\gamma} \sigma_n^{-,\text{in}}(t) \quad (3a)$$

$$\dot{a} = -(i\delta_c + \gamma_c) a - ig \sum_{n=1}^N \sigma_n^- + \sqrt{2\gamma_c} a^{-,\text{in}}(t) \quad (3b)$$

$$\dot{b}_n = -(i\omega_{\text{vib}} + \Gamma) b_n + i\lambda \omega_{\text{vib}} \sigma_n^+ \sigma_n^- + \sqrt{2\Gamma} b_n^{-,\text{in}}(t) \quad (3c)$$

where the noise operators $\sigma_n^{-,\text{in}}(t)$, $a^{-,\text{in}}(t)$, $b_n^{-,\text{in}}(t)$ obey the fluctuation-dissipation relation

$$\langle b_j^{\text{in},\dagger}(t) b_{j'}^{\text{in}}(t') \rangle = \bar{n}_{\text{th}} \delta_{jj'} \delta(t - t'), \quad \langle b_j^{\text{in}}(t) b_{j'}^{\text{in},\dagger}(t') \rangle = (\bar{n}_{\text{th}} + 1) \delta_{jj'} \delta(t - t') \quad (4a)$$

$$\langle a^{\text{in},\dagger}(t) a^{\text{in}}(t') \rangle = 0, \quad \langle a^{\text{in}}(t) a^{\text{in},\dagger}(t') \rangle = \delta(t - t') \quad (4b)$$

$$\langle \sigma_j^{\text{in},+}(t) \sigma_{j'}^{\text{in},-}(t') \rangle = 0, \quad \langle \sigma_j^{\text{in},-}(t) \sigma_{j'}^{\text{in},+}(t') \rangle = \langle \sigma_j^- \sigma_{j'}^+ \rangle \delta_{jj'} \delta(t - t'). \quad (4c)$$

We apply the polaron transform to diagonalize the molecular Hamiltonian apart from the photon degrees of freedom

$$D = \otimes \prod_{n=1}^N D_n, \quad D_n = e^{\lambda(b_n - b_n^\dagger)}. \quad (5)$$

Defining the dressed lowering operator: $\tilde{\sigma}_n^- = \sigma_n^- D_n^\dagger$, one has

$$\dot{D}_n = \lambda D_n [i\omega_{\text{vib}} (b_n + b_n^\dagger - 2\lambda \sigma_n^+ \sigma_n^-) - \Gamma (b_n^\dagger - b_n) + \sqrt{2\Gamma} (b_n^{\text{in},\dagger}(t) - b_n^{\text{in}}(t))]. \quad (6)$$

Inserting Eq.(6) into Eq.(3a) and taking the time derivative of $\tilde{\sigma}_n^-$, some algebra gives

$$\begin{aligned} \dot{\tilde{\sigma}}_n^- = & - [i(\delta - 2\lambda^2\omega_{\text{vib}}) + \gamma] \tilde{\sigma}_n^- - ig\sigma_n^z a D_n^\dagger - i \sum_{j=1}^3 \sigma_n^z D_n^\dagger \Omega_j(t - T_j) e^{-i(v_j - v_3)t} e^{iv_j T_j} \\ & + \lambda\Gamma (b_n^\dagger - b_n) \tilde{\sigma}_n^- - \lambda\sqrt{2\Gamma} [b_n^{\text{in},\dagger}(t) - b_n^{\text{in}}(t)] \tilde{\sigma}_n^- + \sqrt{2\gamma} \tilde{\sigma}_n^{-,\text{in}}(t) \end{aligned} \quad (7)$$

and $\tilde{\sigma}_n^{-,\text{in}}(t) = \sigma_n^{-,\text{in}} D_n^\dagger$. It turns out that the time dynamics of the population $\tilde{\sigma}_n^+ \tilde{\sigma}_n^-$ eliminates the contribution from the term $\lambda\sqrt{2\Gamma} [b_n^{\text{in},\dagger}(t) - b_n^{\text{in}}(t)]$ such that

$$\dot{n}_l \rightarrow -\lambda\sqrt{2\Gamma} [b_l^{\text{in},\dagger}(t) - b_l^{\text{in}}(t) + \text{h.c.}] n_l = 0. \quad (8)$$

The term $\lambda\sqrt{2\Gamma} [b_n^{\text{in},\dagger}(t) - b_n^{\text{in}}(t)]$ can be properly dropped, for a good approximation. One observes that the nuclear velocity $\propto i(b_n^\dagger - b_n)$ which is much slower than electrons and holes. We may further drop the term correspondingly and neglect the back influence from exciton to nuclear motion, where the latter recasts Eq.(3c) into $\dot{b}_n \approx -(i\omega_{\text{vib}} + \Gamma)b_n + \sqrt{2\Gamma}b_n^{-,\text{in}}(t)$. We then solve for the vibration dynamics

$$b_n(t) \approx e^{-(i\omega_{\text{vib}} + \Gamma)t} b_n(0) + \sqrt{2\Gamma} \int_0^t e^{-(i\omega_{\text{vib}} + \Gamma)(t-t')} b_n^{-,\text{in}}(t') dt' \quad (9)$$

which possess

$$[b_n(t), b_m^\dagger(t')] = \begin{cases} e^{-(i\omega_{\text{vib}} + \Gamma)(t-t')} \delta_{nm}, & \text{for } t \geq t' \\ e^{(i\omega_{\text{vib}} - \Gamma)(t'-t)} \delta_{nm}, & \text{for } t < t'. \end{cases} \quad (10)$$

We recast the QLEs into

$$\dot{\tilde{\sigma}}_l^- = -(i\tilde{\delta} + \gamma)\tilde{\sigma}_l^- - ig\sigma_l^z a D_l^\dagger + i \sum_{j=1}^3 (2n_l - 1) D_l^\dagger \Omega_j(t - T_j) e^{-i(v_j - v_3)t} e^{iv_j T_j} + \sqrt{2\gamma} \tilde{\sigma}_l^{-,\text{in}}(t) \quad (11a)$$

$$\dot{a} = -(i\delta_c + \gamma_c)a - ig \sum_{n=1}^N \tilde{\sigma}_n^- D_n + \sqrt{2\gamma_c} a^{-,\text{in}}(t), \quad \tilde{\delta} \equiv \delta - 2\lambda^2\omega_{\text{vib}} \quad (11b)$$

which can be reformed into a compact form

$$\dot{\mathbf{V}} = -\mathbf{M}\mathbf{V} + \mathbf{V}^{\text{in}}(t) + i \sum_{j=1}^3 \Omega_j(t - T_j) e^{iv_j T_j} e^{-i(v_j - v_3)t} \mathbf{W}_x \quad (12)$$

where the related matrices are

$$\mathbf{V} = \begin{pmatrix} \tilde{\sigma}_1^- \\ \tilde{\sigma}_2^- \\ \vdots \\ \tilde{\sigma}_N^- \\ a \end{pmatrix}, \quad \hat{\mathbf{M}} = \begin{pmatrix} i\tilde{\delta} + \gamma & 0 & \cdots & 0 & ig\sigma_1^z D_1^\dagger \\ 0 & i\tilde{\delta} + \gamma & \cdots & 0 & ig\sigma_2^z D_2^\dagger \\ \vdots & \vdots & \ddots & \vdots & \vdots \\ 0 & 0 & \cdots & i\tilde{\delta} + \gamma & ig\sigma_N^z D_N^\dagger \\ igD_1 & igD_2 & \cdots & igD_N & i\delta_c + \gamma_c \end{pmatrix}, \quad \mathbf{V}^{\text{in}}(t) = \begin{pmatrix} \sqrt{2\gamma} \tilde{\sigma}_1^{-,\text{in}}(t) \\ \sqrt{2\gamma} \tilde{\sigma}_2^{-,\text{in}}(t) \\ \vdots \\ \sqrt{2\gamma} \tilde{\sigma}_N^{-,\text{in}}(t) \\ \sqrt{2\gamma_c} a^{\text{in}}(t) \end{pmatrix}, \quad \mathbf{W}_x = \begin{pmatrix} (2n_1 - 1) D_1^\dagger \\ (2n_2 - 1) D_2^\dagger \\ \vdots \\ (2n_N - 1) D_N^\dagger \\ 0 \end{pmatrix}. \quad (13)$$

We find following identities for the vibrations [1, 2]

$$\begin{aligned} e^{\lambda[b_n^\dagger(t) - b_n(t)]} &= e^{-\lambda^2/2} e^{\lambda b_n^\dagger(t)} e^{-\lambda b_n(t)} = e^{\lambda^2/2} e^{-\lambda b_n(t)} e^{\lambda b_n^\dagger(t)} \\ e^{-\lambda b_n(t)} |0\rangle &= |0\rangle \end{aligned} \quad (14)$$

and $e^A e^B = e^B e^A e^{[A,B]}$, given $[[A,B], A] = [[A,B], B] = 0$ from the Baker-Hausdorff formula. Eq.(9) thus enables us to calculate the vibration correlation functions. For instance, the two-point correlator reads

$$\begin{aligned} e^{\lambda^2} \langle 0 | D_i^\dagger(t) D_j(t') | 0 \rangle &= \langle 0 | e^{\lambda b_i(t)} e^{\lambda b_j^\dagger(t')} | 0 \rangle \\ &= \langle 0 | e^{\lambda b_j^\dagger(t')} e^{\lambda b_i(t)} e^{\lambda^2 [b_i(t), b_j^\dagger(t')]} | 0 \rangle \\ &= \theta(t - t') \exp \left[\delta_{ij} \lambda^2 e^{-(i\omega_{\text{vib}} + \Gamma)(t-t')} \right] + \theta(t' - t) \exp \left[\delta_{ij} \lambda^2 e^{(i\omega_{\text{vib}} - \Gamma)(t'-t)} \right]. \end{aligned} \quad (15)$$

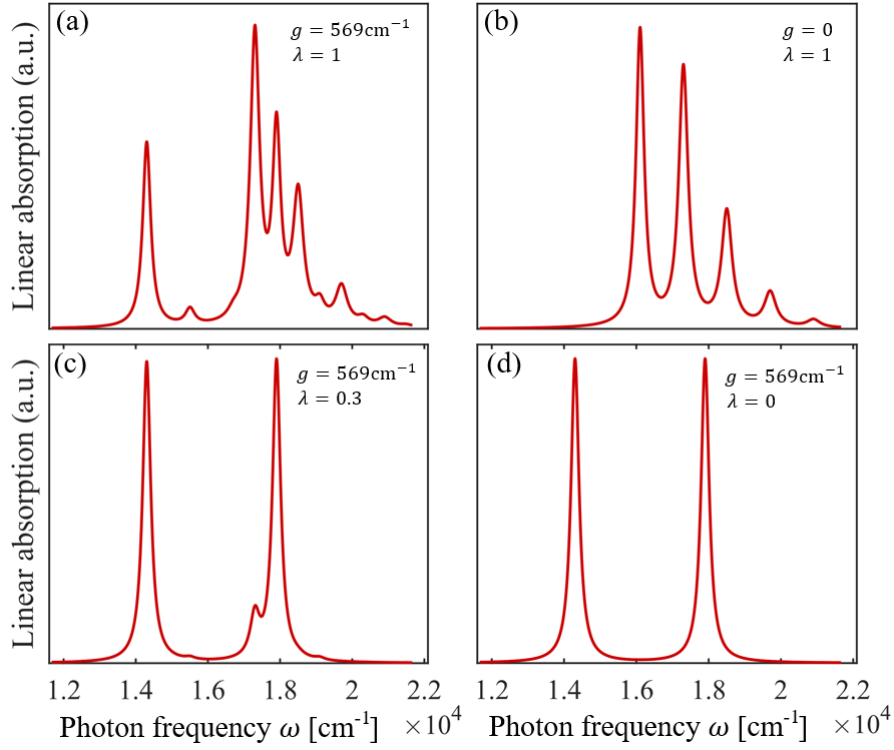


FIG. 1: Linear absorption spectrum of molecular polaritons with $N = 10$ organic molecules in an optical cavity, with different exciton-photon and vibronic couplings. The parameters are taken to be $\omega_n = 16113\text{cm}^{-1}$, $\tilde{\delta} = \delta_c = 0$, $\Gamma = 20\text{cm}^{-1}$, $\gamma = 1\text{cm}^{-1}$, $\gamma_c = 0.9\text{cm}^{-1}$, $\omega_{\text{vib}} = 1200\text{cm}^{-1}$, typically from cyanine dyes [3].

The four-point correlator is calculated in further

$$\begin{aligned}
& e^{2\lambda^2} \langle 0 | D_{j'}(t) D_j^\dagger(t') D_l^\dagger(t'') D_i(t''') | 0 \rangle \\
&= \langle 0 | e^{-\lambda b_{j'}(t)} e^{-\lambda b_j^\dagger(t')} e^{\lambda b_j(t')} e^{-\lambda b_l^\dagger(t'')} e^{\lambda b_l(t'')} e^{\lambda b_i^\dagger(t''')} | 0 \rangle \\
&= e^{\lambda^2 [b_{j'}(t), b_j^\dagger(t')]} e^{\lambda^2 [b_l(t''), b_l^\dagger(t''')]} \langle 0 | e^{-\lambda b_{j'}(t)} e^{\lambda b_j(t')} e^{-\lambda b_l^\dagger(t'')} e^{\lambda b_l^\dagger(t''')} | 0 \rangle \\
&= e^{\lambda^2 [b_{j'}(t), b_j^\dagger(t')]} e^{\lambda^2 [b_l(t''), b_l^\dagger(t''')]} e^{-\lambda^2 [b_j(t'), b_l^\dagger(t'')]} e^{\lambda^2 [b_{j'}(t), b_l^\dagger(t'')]} e^{\lambda^2 [b_j(t'), b_l^\dagger(t''')]} e^{-\lambda^2 [b_{j'}(t), b_l^\dagger(t''')]}
\end{aligned} \tag{16}$$

which is general. For the segment $t \leq t' \leq t'' \leq t'''$, it reads

$$\begin{aligned}
& e^{2\lambda^2} \langle 0 | D_{j'}(t) D_j^\dagger(t') D_l^\dagger(t'') D_i(t''') | 0 \rangle \theta(t''' - t'') \theta(t'' - t') \theta(t' - t) \\
&= \exp \left[\lambda^2 \delta_{j'j} e^{(i\omega_{\text{vib}} - \Gamma)(t' - t)} \right] \exp \left[\lambda^2 \delta_{il} e^{(i\omega_{\text{vib}} - \Gamma)(t''' - t'')} \right] \exp \left[-\lambda^2 \delta_{jl} e^{(i\omega_{\text{vib}} - \Gamma)(t'' - t')} \right] \\
&\quad \times \exp \left[\lambda^2 \delta_{j'l} e^{(i\omega_{\text{vib}} - \Gamma)(t'' - t)} \right] \exp \left[\lambda^2 \delta_{ij} e^{(i\omega_{\text{vib}} - \Gamma)(t''' - t')} \right] \exp \left[-\lambda^2 \delta_{ij'} e^{(i\omega_{\text{vib}} - \Gamma)(t''' - t)} \right].
\end{aligned} \tag{17}$$

For the other 23 segments, the calculations proceed as above by using Eq.(10). The results will be presented elsewhere. Eq.(16) will be useful for calculating the 3rd-order signals entailed later.

ABSORPTION AND EMISSION SPECTRA

Using Eq.(12) it is straightforward to find the solution to the 1st order with respect to the external field. The n_j in W_x is responsible for the emission whereas the 1 in W_x is for absorption. Subject to a probe pulse, Eq.(12) yields

the 1st-order solution

$$V_1(t) = i \int_0^t \Omega(\tau - T) e^{ivT} G(t - \tau) W_x(\tau) d\tau. \quad (18)$$

The far-field polarization of cavity polaritons thus reads

$$P_A(t) = -i |\mu_{eg}|^2 \sum_{i=1}^N \sum_{l=1}^N \int_{-\infty}^t d\tau E(\tau - T) e^{-iv(\tau - T)} \langle 0 | G_{il}(t - \tau) D_i(t) D_l^\dagger(\tau) | 0 \rangle \quad (19a)$$

$$P_E(t) = 2i |\mu_{eg}|^2 \sum_{i=1}^N \sum_{l=1}^N \int_{-\infty}^t d\tau E(\tau - T) e^{-iv(\tau - T)} \langle 0 | G_{il}(t - \tau) n_l(\tau) D_l^\dagger(\tau) D_i(t) | 0 \rangle \quad (19b)$$

for absorption and emission components, while the Fourier transform of Eq.(19b) gives Eq.(6) in main text. The propagator $G(t)$ is of the same form as the one given in main text. Eq.(19a) defines the 1st-order response function $\chi^{(1)}(\omega)$ through the Fourier component of the $P_A(t)$

$$\chi^{(1)}(\omega) = |\mu_{eg}|^2 \left[\sum_{k=1}^{N+1} \frac{\left(\sum_{i=1}^N T_{ik} \right) \left(\sum_{l=1}^N T_{kl}^{-1} \right) e^{-\lambda^2}}{\omega - \omega_k + i\gamma_k} + \sum_{k=1}^{N+1} \sum_{m=1}^{\infty} \frac{\left(\sum_{l=1}^N T_{lk} T_{kl}^{-1} \right) S_m^\lambda}{\omega - \omega_k - m\omega_{\text{vib}} + i(\gamma_k + m\Gamma)} \right] \quad (20)$$

and $S_m^\lambda = e^{-\lambda^2} \lambda^{2m} / m!$ is the Franck-Condon factor [4, 5]. The 1st term in Eq.(20) indicates the polaritons while the peak vanishes as $k = \text{Dark}$. The 2nd term indicates the emitter dark states (EDSs) decoupled from the cavity photons, responsible for the breakdown of the cooperativity in the cavity polaritons and dark states. To see the absorption closely, we can assume $\gamma = \gamma_c$, $\tilde{\delta} = \delta_c = 0$ in the M matrix, which results in $T^{-1} = T^\dagger$. We can solve for the T matrix, having $\sum_{l=1}^N T_{lk} = 0$, $|T_{lk}|^2 = 1/N$ for $k = \text{Dark}$ and $\sum_{l=1}^N T_{lk} = \sqrt{N/2}$, $\sum_{l=1}^N |T_{lk}|^2 = 1/2$ for $k = \text{LP}$ and UP . For a few certain modes, i.e., $\omega = \omega_{\text{LP/UP}}$, $\omega_{\text{LP/UP}} + m\omega_{\text{vib}}$, $\omega_D + m\omega_{\text{vib}}$, the peak intensities can be found accordingly which yields the ratios

$$\frac{S_A(\omega_D + m\omega_{\text{vib}})}{S_A(\omega_{\text{LP/UP}})} = \frac{\lambda^{2m}}{m!} \left(1 - \frac{1}{N} \right) \frac{2\gamma_{\text{LP/UP}}}{\gamma_D + m\Gamma} \approx 2 \frac{\lambda^{2m}}{m!} \frac{\gamma_{\text{LP/UP}}}{m\Gamma} \quad \text{as } N \gg 1 \quad (21a)$$

$$\frac{S_A(\omega_{\text{LP/UP}} + m\omega_{\text{vib}})}{S_A(\omega_{\text{LP/UP}})} = \frac{\lambda^{2m}}{m!N} \frac{\gamma_{\text{LP/UP}}}{\gamma_{\text{LP/UP}} + m\Gamma} \approx 0 \quad \text{as } N \gg 1. \quad (21b)$$

Between the two polariton states, we can observe an extra peak at $\omega_D + \omega_{\text{vib}}$ supporting an EDS that results from the vibronic coupling quantified by the Frank-Condon factor. This is evident by Eq.(21a), indicating the EDSs decoupled from the cavity photons and the large oscillator strength owing to the density of states $\sim N$ shown in Fig.1(a). The properties of EDSs can be further seen from Fig.1(b) for the case when turning off the cavity, as a benchmark to strong-coupling cases. For weaker vibronic coupling, as shown in Fig.1(c,d), the EDSs are masked by the Rabi splitting that evidences the strong molecular cooperativity. Therefore the EDSs reveal the polariton-induced cooperativity between molecules broken by the vibration fluctuations. As will be shown, the polariton dynamics against the EDSs, for a deeper understanding of molecular cooperativity, can be monitored by the multidimensional projections of the signal.

TWO-DIMENSIONAL COHERENT SIGNAL

To find the two-dimensional spectroscopic signal, we are seeking the solution in series of the molecule-field interactions, i.e., $V = V_0 + V_1 + V_2 + V_3 + \dots$. The 0th-order term V_0 is a result of free propagation in the absence of classical pulses, while the 1st-order term denotes the absorption under the pulse 1, creating the coherence between the ground and electronically excited states. Namely, it reads

$$V_0(t) = G(t)V(0) + i \int_0^t G(t - t') V^{\text{in}}(t') dt' \quad (22a)$$

$$V_1(t) = -i \sum_{s=1}^3 \int_0^t dt' \Omega_s(t' - T_s) e^{iv_s T_s} G(t - t') \bar{W}(t') e^{-i(v_s - v_3)t'} \quad (22b)$$

and $\bar{W}(t') = [D_1^\dagger(t'), D_2^\dagger(t'), \dots, D_N^\dagger(t'), 0]^\top$, which yield the electronic polarization to the 1st order

$$\bar{\sigma}_{i;1}^-(t) = -i \sum_{s=1}^3 \sum_{j=1}^N \int_0^t dt' \Omega_s(t' - T_s) e^{iv_s T_s} G_{lj}(t - t') D_j^\dagger(t') e^{-i(v_s - v_3)t'}. \quad (23)$$

Knowing that the excitations are produced by the first two pulses, one has $n_{l;2}(t) = \sigma_{l;1}^+(t) \sigma_{l;1}^-(t)$, yielding

$$n_{l;2}(t) = \sum_{j=1}^N \sum_{j'=1}^N \int_0^t dt'' \int_0^{t''} dt' \Omega_1^*(t' - T_1) \Omega_2(t'' - T_2) e^{-i(v_1 T_1 - v_2 T_2)} e^{-i(v_3 - v_1)t'} e^{i(v_3 - v_2)t''} \\ \times G_{lj'}^*(t - t') G_{lj}(t - t'') D_{j'}(t') D_j^\dagger(t'') + [\text{Other combinations}]. \quad (24)$$

It is obvious that the 2nd-order correction $V_2(t)$ must involve the noise operators in the form of $\tilde{\sigma}_i^{\pm, \text{in}}(t)$ and $\tilde{\sigma}_i^{+, \text{in}}(t) \tilde{\sigma}_j^-, \text{in}}(t') \tilde{\sigma}_k^-, \text{in}}(t'')$ + their Hermitian conjugates. Proceeding to the 3rd-order correction, the noise-operator-dependent terms remain the combinations $\tilde{\sigma}_i^{+, \text{in}}(t) \tilde{\sigma}_j^-, \text{in}}(t') \tilde{\sigma}_k^+, \text{in}}(t'') \tilde{\sigma}_l^-, \text{in}}(t''')$ as well as $\tilde{\sigma}_i^{+, \text{in}}(t) \tilde{\sigma}_j^+, \text{in}}(t') \tilde{\sigma}_k^-, \text{in}}(t'') \tilde{\sigma}_l^-, \text{in}}(t''')$. These will not contribute to the 3rd-order signals eventually, by noting

$$\langle \tilde{\sigma}_i^{+, \text{in}}(t) \tilde{\sigma}_j^-, \text{in}}(t') \tilde{\sigma}_k^+, \text{in}}(t'') \tilde{\sigma}_l^-, \text{in}}(t''') \rangle = 0, \quad \langle \tilde{\sigma}_i^{+, \text{in}}(t) \tilde{\sigma}_j^+, \text{in}}(t') \tilde{\sigma}_k^-, \text{in}}(t'') \tilde{\sigma}_l^-, \text{in}}(t''') \rangle = 0 \quad (25)$$

given $\langle \tilde{\sigma}_i^{+, \text{in}}(t) \tilde{\sigma}_j^-, \text{in}}(t') \rangle = 0$. This is reasonable because creating the excitons via environmental fluctuations is of extremely low chance, at room temperature. Keeping the significant components for the signals, we have $V_2(t) = 0$ therein, by noting the fact $V(0) = 0$ prior to the pulse action. We therefore proceed to the 3rd-order correction via Eq.(12) and (24), obtaining

$$V_3(t) = 2i \int_0^t d\tau \Omega_3(\tau - T_3) e^{iv_3 T_3} G(t - \tau) W_y(\tau) + [\text{Other combinations}] \quad (26)$$

where $W_y(\tau) = [n_{1;2}(\tau) D_1^\dagger(\tau), n_{2;2}(\tau) D_2^\dagger(\tau), \dots, n_{N;2}(\tau) D_N^\dagger(\tau), 0]^\top$. As the three pulses are time-ordered, the transition pathways are selective. This enables us to simplify the 3rd-order polarization of molecules, resulting from the term cancellation. Along the direction $\mathbf{k}_I = -\mathbf{k}_1 + \mathbf{k}_2 + \mathbf{k}_3$, the far-field dipolar radiation reads from Eq.(26)

$$\sigma_{i;3}^-(t) = 2i \sum_{l=1}^N \int_0^t d\tau \Omega_3(\tau - T_3) e^{-iv_3(t - T_3)} G_{il}(t - \tau) n_{l;2}(\tau) D_l^\dagger(\tau) D_i(t). \quad (27)$$

So far, we have derived in a math rigor the 3rd-order polarization of molecules, keeping all the essential terms. Thus Eq.(27) must contain the transient absorption component, provided that the eigenvalues of the matrix \hat{M} normally involve the frequencies corresponding to the higher transition ladders, i.e., $e \rightarrow f$. This is an important aspect for a self-consistent formalism of the spectroscopic signals, as the ultrashort pulses having broad bandwidth would induce considerably the transitions to the doubly-excited manifold. For instance, a large number of identical molecules that may enable the approximation $g\sigma_i^z \approx g$ when including up to the doubly-excited manifold (applicable for few-photon cavities), the cascading transitions $g \rightarrow e$, $e \rightarrow f$ will have the same frequencies. This can be seen from the eigenvalues of the \hat{M} , given no direct many-particle couplings between molecules.

Inserting Eq.(24) into Eq.(27) and carrying out the Fourier transform we obtain the macroscopic far-field polarization $P(t) = \mu_{eg}^* \sum_{i=1}^N \langle \sigma_{i;3}^-(t) \rangle$ which yields

$$P(\omega) = 2i\mu_{eg}^* \sum_{i,l=1}^N \sum_{j,j'=1}^N \sum_{m=1}^{N+1} \int_{-\infty}^{\infty} dt \int_0^t d\tau \int_0^\tau dt'' \int_0^{t''} dt' e^{i\omega T_3} e^{i(\omega - v_3)(t - T_3)} e^{iv_3(t'' - t')} e^{-iv_2(t'' - T_2)} \\ \times e^{iv_1(t' - T_1)} \Omega_3(\tau - T_3) \Omega_2(t'' - T_2) \Omega_1^*(t' - T_1) \langle 0 | G_{il}(t - \tau) G_{lm}^*(\tau - t'') \\ \times G_{lj}(\tau - t'') G_{mj'}^*(t'' - t') D_{j'}(t') D_j^\dagger(t'') D_l^\dagger(\tau) D_i(t) | 0 \rangle \\ = 2i\mu_{eg}^* \Omega_3 \Omega_2 \Omega_1^* \sum_{i,l=1}^N \sum_{j,j'=1}^N \sum_{m=1}^{N+1} \int_{T_3}^{\infty} dt e^{i\omega T_3} e^{i(\omega - v_3)(t - T_3)} e^{iv_3(T_2 - T_1)} \langle 0 | G_{il}(t - T_3) G_{lm}^*(T_3 - T_2) \\ \times G_{lj}(T_3 - T_2) G_{mj'}^*(T_2 - T_1) D_{j'}(T_1) D_j^\dagger(T_2) D_l^\dagger(T_3) D_i(t) | 0 \rangle \quad (28)$$

where the last step invokes the *impulsive approximation*, i.e., $\Omega_i(t - T_i) \simeq \Omega_i \delta(t - T_i)$ [1, 6]. Using Eq.(10) and (16), the vibrational correlation function can be evaluated

$$\begin{aligned}
& \langle 0 | D_{j'}(T_1) D_j^\dagger(T_2) D_l^\dagger(T_3) D_i(t) | 0 \rangle \\
&= e^{-2\lambda^2} \exp \left[\lambda^2 \delta_{j'j} e^{(i\omega_{\text{vib}} - \Gamma)(T_2 - T_1)} \right] \exp \left[\lambda^2 \delta_{il} e^{(i\omega_{\text{vib}} - \Gamma)(t - T_3)} \right] \exp \left[-\lambda^2 \delta_{jl} e^{(i\omega_{\text{vib}} - \Gamma)(T_3 - T_2)} \right] \\
&\quad \times \exp \left[\lambda^2 \delta_{j'l} e^{(i\omega_{\text{vib}} - \Gamma)(T_3 - T_1)} \right] \exp \left[\lambda^2 \delta_{ij} e^{(i\omega_{\text{vib}} - \Gamma)(t - T_2)} \right] \exp \left[-\lambda^2 \delta_{ij'} e^{(i\omega_{\text{vib}} - \Gamma)(t - T_1)} \right] \\
&= e^{4\lambda^2} \sum_{m_1=0}^{\infty} \sum_{m_2=0}^{\infty} \sum_{m_3=0}^{\infty} \sum_{m_4=0}^{\infty} \sum_{m_5=0}^{\infty} \sum_{m_6=0}^{\infty} S_{m_1}^\lambda S_{m_2}^\lambda S_{m_3}^\lambda S_{m_4}^\lambda S_{m_5}^\lambda S_{m_6}^\lambda (-1)^{m_3+m_6} \delta_{j'j}^{m_1} \delta_{il}^{m_2} \delta_{jl}^{m_3} \delta_{j'l}^{m_4} \delta_{ij}^{m_5} \delta_{ij'}^{m_6} \\
&\quad \times e^{(m_2+m_5+m_6)(i\omega_{\text{vib}} - \Gamma)(t - T_3)} e^{(m_3+m_4+m_5+m_6)(i\omega_{\text{vib}} - \Gamma)(T_3 - T_2)} e^{(m_1+m_4+m_6)(i\omega_{\text{vib}} - \Gamma)(T_2 - T_1)}
\end{aligned} \tag{29}$$

with $T_1 < T_2 < T_3 < t$. Inserting Eq.(29) into Eq.(28), the polarization can be obtained. The heterodyne-detected signal is $S(\omega, T, \omega_e) = \int_0^\infty E_{\text{LO}}^*(\omega) P(\omega) e^{i\omega_e \tau} d\tau$, where $E_{\text{LO}}(\omega)$ is the Fourier component of the reference beam. Thus

$$\begin{aligned}
S(\omega, T, \omega_e) &= -i |\mu_{eg}|^4 E_{\text{LO}}^* E_3 E_2 E_1^* \sum_{i,l=1}^N \sum_{j,j'=1}^N \sum_{p=1}^{N+1} \sum_{k_1,k_2=1}^{N+1} \sum_{\{m\}=0}^{\infty} e^{4\lambda^2} S_{m_1}^\lambda S_{m_2}^\lambda S_{m_3}^\lambda S_{m_4}^\lambda S_{m_5}^\lambda S_{m_6}^\lambda (-1)^{m_3+m_6} \\
&\quad \times \frac{\delta_{j'j}^{m_1} \delta_{il}^{m_2} \delta_{jl}^{m_3} \delta_{j'l}^{m_4} \delta_{ij}^{m_5} \delta_{ij'}^{m_6} T_{i,k_1} T_{k_1,l}^{-1}}{\omega - \omega_{k_1} + (m_2 + m_5 + m_6)\omega_{\text{vib}} + i[\gamma_{k_1} + (m_2 + m_5 + m_6)\Gamma]} G_{lp}^*(T) G_{lj}(T) \\
&\quad \times e^{(m_3+m_4+m_5+m_6)(i\omega_{\text{vib}} - \Gamma)T} \frac{T_{p,k_2}^* T_{k_2,j'}^{-1,*}}{\omega_e + \omega_{k_2} + (m_1 + m_4 + m_6)\omega_{\text{vib}} + i[\gamma_{k_2} + (m_1 + m_4 + m_6)\Gamma]}.
\end{aligned} \tag{30}$$

The signal measured in detectors is $S_{2\text{D}}(\omega, T, \omega_e) = \text{Im}[S(\omega, T, \omega_e)]$.

ULTRAFAST PUMP-PROBE SIGNAL

To monitor the polariton dynamics of molecular ensembles, a pump-probe technique composing two broadband pulses with a time delay may be an alternative signal. This acquires the far-field polarization involving the 3rd-order expansion in the field-molecule interaction, as what has been done for the multidimensional signal. The procedures emulate the one for the multidimensional signal entailed before, so that we will present the most significant terms to avoid redundancy, with the rigorous math given in previous section. Invoking the *impulsive* approximation in regard of the ultrashort pulses, i.e., $\Omega_i(t - T_i) \approx \Omega_i \delta(t - T_i)$, the vibration correlation function is found to be

$$\begin{aligned}
\langle 0 | D_{j'}(T_1) D_j^\dagger(T_1) D_l^\dagger(T_3) D_i(t) | 0 \rangle &= e^{-2\lambda^2} \exp \left[\lambda^2 \delta_{il} e^{(i\omega_{\text{vib}} - \Gamma)(t - T_3)} \right] \exp \left[\lambda^2 (\delta_{j'l} - \delta_{jl}) e^{(i\omega_{\text{vib}} - \Gamma)(T_3 - T_1)} \right] \\
&\quad \times \exp \left[\lambda^2 (\delta_{ij} - \delta_{ij'}) e^{(i\omega_{\text{vib}} - \Gamma)(t - T_1)} \right] \\
&= e^{\lambda^2} \sum_{m_1}^{\infty} \sum_{m_2}^{\infty} \sum_{m_3}^{\infty} S_{m_1}^\lambda S_{m_2}^\lambda S_{m_3}^\lambda \delta_{il}^{m_1} (\delta_{j'l} - \delta_{jl})^{m_2} (\delta_{ij} - \delta_{ij'})^{m_3} \\
&\quad \times e^{(m_1+m_3)(i\omega_{\text{vib}} - \Gamma)(t - T_3)} e^{(m_2+m_3)(i\omega_{\text{vib}} - \Gamma)(T_3 - T_1)}
\end{aligned} \tag{31}$$

where T_1 and T_3 denote the arrival time of pump and probe pulses, respectively. The time delay follows $T = T_3 - T_1$. The macroscopic polarization can be found correspondingly, through substituting Eq.(31) into (28). The signal measured in pump-probe experiments is the transmission of the probe field with a time grating, i.e., $S_{\text{pp}}(\omega, T) = \text{Im}[E_3^*(\omega) P(\omega)]$. Accounting for the non-rephasing component with similar manipulations, one reaches the full pump-

probe signal

$$S_{\text{pp}}(\omega, T) = -4|\mu_{eg}|^4|E_3|^2|E_1|^2 \sum_{i,l=1}^N \sum_{j,j'=1}^N \sum_{k=1}^{N+1} \sum_{m_1=0}^{\infty} \sum_{m_2=0}^{\infty} \sum_{m_3=0}^{\infty} e^{\lambda^2} S_{m_1}^{\lambda} S_{m_2}^{\lambda} S_{m_3}^{\lambda} \delta_{il}^{m_1} (\delta_{j'l} - \delta_{jl})^{m_2} \times (\delta_{ij} - \delta_{ij'})^{m_3} \text{Im} \left[\frac{T_{ik} T_{kl}^{-1} G_{lj'}^*(T) G_{lj}(T) e^{(m_2+m_3)(i\omega_{\text{vib}}-\Gamma)T}}{\omega - \omega_k + (m_1 + m_3)\omega_{\text{vib}} + i(\gamma_k + (m_1 + m_3)\Gamma)} \right]. \quad (32)$$

The ultrafast pump-probe signal may reveal the collective dynamics of cavity polaritons via simulating Eq.(32). This is straightforward but is not quite necessary, as the pump-probe signal has simpler form from which some generic features can be observed for polariton dynamics. We will work for the sake of generality, to manifest the the time-resolved signal generically. The broadband nature of the ultrashort pulses causes no selective mode absorption in molecular polaritons, whereas the time grating makes the emission spectrally resolved. At zero delay, Eq.(32) resolves the LP and UP modes separated by $2g\sqrt{N}$, and also the EDSs at $\omega = \omega_D - \omega_{\text{vib}}, \omega_D - 2\omega_{\text{vib}}, \dots$. The peak intensity distribution over the modes follows the absorption spectrum in Eq.(20), apart from the Stokes shifts of (*negative integer*) $\times \omega_{\text{vib}}$ instead of the anti-Stokes shifts. This takes the rational from recalling the absorption and fluorescence spectrums in molecular spectroscopy [1, 7]. By varying the time delay such that $T > 0$, the fast relaxation towards the EDSs can be monitored from the dramatic change of the peak intensities at $\omega = \omega_D - m\omega_{\text{vib}}$, i.e.,

$$S_{\text{pp}}(\omega_{\text{UP}}, T) \propto \frac{e^{-\lambda^2}}{2\gamma_{\text{UP}}} \sum_{l=1}^N \sum_{j,j'=1}^N \sum_{m=0}^{\infty} S_m^{\lambda} (\delta_{j'l} - \delta_{jl})^m \text{Re} \left[G_{lj'}^*(T) G_{lj}(T) e^{m(i\omega_{\text{vib}}-\Gamma)T} \right] \quad (33a)$$

$$S_{\text{pp}}(\omega_D - (m_1 + m_3)\omega_{\text{vib}}, T) \propto \frac{e^{\lambda^2}}{N} \sum_{s,l=1}^N \sum_{j,j'=1}^N \sum_{m_2=0}^{\infty} \frac{S_{m_1}^{\lambda} S_{m_2}^{\lambda} S_{m_3}^{\lambda} \delta_{sl}^{m_1} (\delta_{j'l} - \delta_{jl})^{m_2} (\delta_{sj} - \delta_{sj'})^{m_3}}{\gamma_k + (m_1 + m_3)\Gamma} \times \text{Re} \left[e^{i(\phi_{sk} + \phi_{kl})} G_{lj'}^*(T) G_{lj}(T) e^{(m_2+m_3)(i\omega_{\text{vib}}-\Gamma)T} \right]. \quad (33b)$$

Eq.(27) evidences the coherent energy transfer and exchange between polariton states and EDSs, from the phase factor $e^{i(\phi_{sk} + \phi_{kl})}$ in Eq.(33b) associated with different damping rates that are responsible for the incoherent channels of relaxation of EDSs. $\phi_{sk} = e^{-2\pi is(k-1)/N}$ for molecules placed in a cavity with a linear fashion along the cavity axis. One would expect in further the π phase difference between the time-evolving dynamics of UP/LP and EDSs, for properly-chosen parameters. Because of the density of states $\sim N$ for EDSs, higher than the one for polaritons, the EDSs show the localized nature. The polariton states featuring the extended waves are therefore trading off with the EDS-induced localization, as indicated from Eq.(33a) and Eq.(33b) showing multiple channels and timescales for the relaxation processes. The pump-probe signal, however, cannot provide more detailed information in this regard. Advanced information about the polariton dynamics against the EDSs, for a deeper understanding of molecular cooperativity and relaxations of polaritons and dark states, can be learned from extending the pump-probe scheme to multidimensional projections of the signal.

* zzhan26@cityu.edu.hk

† smukamel@uci.edu

- [1] S. Mukamel, *Principles of Nonlinear Optical Spectroscopy* (Oxford University Press, Oxford, 1999)
- [2] M. O. Scully and M. S. Zubairy, *Quantum Optics*, 1st ed. (Cambridge University Press, Cambridge, 1997)
- [3] C. A. Guarín, J. P. Villabona-Monsalve, R. López-Arteaga and J. Peon, *J. Phys. Chem. B* **117**, 7352-7362 (2013)
- [4] J. Franck, *Trans. Faraday Soc.* **21**, 536-542 (1925)
- [5] K. Huang and A. Rhys, *Proc. R. Soc. A* **204**, 406-423 (1950)
- [6] Y. J. Yan and S. Mukamel, *J. Chem. Phys.* **94**, 179-190 (1990)
- [7] Y. J. Yan and S. Mukamel, *Phys. Rev. A* **41**, 6485-6504 (1990)